Oil Shale, 2026, 43, 3, 321–334 https://doi.org/10.3176/oil.2026.3.05

Kerogen destruction and partial transfer of metals to shale oil: detection and quantification

Omar S. Al-Ayed[(a)]*, Omar Loai Alnsour[(b)], Eyad S. M. Abu-Nameh[(b)]

[(a)] Department of Chemical Engineering, Faculty of Engineering Technology, Al-Balqa Applied University, Amman Marka 11134, Jordan
[(b)] Department of Chemistry, Faculty of Science, Al-Balqa Applied University, As-Salt 19117, Jordan

Received 2 February 2026, accepted 1 July 2026, available online 3 August 2026

Abstract. *Oil shale is pyrolyzed to investigate the transfer of selected metals (Fe, V, Ni, Mn, and Pb) to shale oil. Several heating rates are employed to study the transfer process during the heating of oil shale under a nitrogen environment. The migration or transfer of Fe, V, Ni, Mn, and Pb from oil shale to shale oil is investigated. These metals are redistributed between shale oil and spent shale. The transfers are studied as a function of heating rates of 5, 10, 15, and 20 °C/min. Metals embedded in oil shale are found to be transferable to shale oil during pyrolysis. The Fe concentration levels in shale oil are 59.4, 35.69, 34.14, and 25.29 ppm at 5, 10, 15, and 20 °C/min, respectively. The transfer of Fe shows a decreasing trend with heating rate. The concentrations of As in shale oil are 10.09, 13.88, 12.2, and 11.04 ppm, showing a decreasing trend at 10, 15, and 20 °C/min. On the other hand, the percentage recovery of Fe is > 93.6% and < 109.3%, while that of As is > 79.3% and < 83.99%. The concentrations of Mn and Pb in shale oil are < 1 ppm. The concentration of Ni in shale oil is < 6.04 ppm at 10 °C/min, whereas it decreases to 3.14 ppm at 20 °C/min. The percentage recovery of Ni ranges from > 81.48 to < 84.13. Finally, low concentrations of V in shale oil are detected. These concentrations are 1.13, 1.45, 0.77, and 1.76 ppm at 5, 10, 15, and 20 °C/min, respectively. The percentage recovery of V is > 76.88% and < 86.31%.*

Keywords: *shale oil, heating rate, metals transfer, oil shale, metals migration.*

1. Introduction

Shale oil is an unconventional condensed liquid hydrocarbon product obtained from the oil shale pyrolysis process [1–2]. Kerogen, the organic portion of

* Corresponding author, omar.alayed@bau.edu.jo

the oil shale, decomposes to hydrocarbon vapors, incondensable gases, and retorted water if subjected to pyrolysis in the temperature range of 350 to 550 °C. The gaseous hydrocarbons generated include CH_4, C_2H_6, C_2H_4, C_3H_8, C_3H_6, n-C_4H_{10}, i-C_4H_{10}, C_4H_8 isomers, and traces of light hydrocarbons. These gases are condensable at room temperature and pyrolysis product condensation conditions. Hydrogen gas and other non-condensable gases such as NO, NO_2, SO_2, CO, CO_2, H_2S, and NH_3 are also generated depending upon the oil shale origin and reaction conditions [3]. On the other hand, different hydrocarbon classes that make up shale oil are also found. These classes include aliphatics (alkanes, alkenes, alkynes, and cycloalkanes), aromatics (benzoids and non-benzoids), and asphaltenes (the insoluble fraction in normal n-alkanes, but soluble in toluene and benzene) [4–7]. The density of the produced shale oil varies between 0.9587 and 0.9974 g/cm^3 [8, 9]. Oja et al. [9] reported that the densities for kukersite, Kashpir, and Green River shale oils increased with increasing boiling point from 0.7055 to 0.9887 g/cm^3, 0.8649 to 1.0031 g/cm^3, and 0.8276 to 0.9506 g/cm^3, respectively. El-Lajjun and Sultani shale oils were reported to have average densities of 0.9668 and 0.964 g/cm^3, respectively [10].

Jordanian oil shale contains several metals as confirmed by XRF results [11]. The XRF analysis of Attarat, Sultani, and El-Lajjun oil shales confirmed the presence of various metals such as Ni, V, Mn, Fe, As, and Pb, as reported by several authors [11–14]. The concentrations of these elements range from below 1 ppm up to about 1000 ppm. Very few researchers have studied the possible transfer of some of these elements to shale oil [15–17]. In a study by Abu-Nameh et al. [17], the transfer of 20 elements was detected in shale oil produced from El-Lajjun, Sultani, and Attarat oil shales. The most transferred element was Fe, followed by Zn, V, As, Cr, and Pb. In a separate study by Wang et al. [18], it was found that Pb transferred to water during in-situ pyrolysis, and it was reported that the rate of transfer increased with increasing temperature. This is an indication that shale oil metals get affected by the pyrolysis conditions and migrate into liquid products such as shale oil and chemical water. Liu et al. [19] studied the volatility of some elements during coal pyrolysis and reported that fuel characteristics depend upon pyrolysis conditions such as final pyrolysis temperature, heating rate, and pyrolysis environment. Migration of trace elements during Mongolian oil shale pyrolysis was investigated by Bai et al. [20]. They found that the rate of heavy metals decreases with increasing specific surface area due to the progress of the pyrolysis process. The developed pores during pyrolysis contributed to the re-adsorption of the released heavy metal elements originating from kerogen thermal cracking. The migration of trace elements in oil shale during pyrolysis is related both to their content and to the final pyrolysis temperature.

The presence of metals in oil shale as a part of ore or as oxides affects the secondary reactions of the generated hydrocarbon vapors. During the pyrolysis process, kerogen molecules crack to give hydrocarbon vapors,

which upon condensation produce shale oil. During the generation process and the transport of these products, the ore or metal oxides influence chemical reactions. The inert gas in the reaction environment and the residence time of the generated hydrocarbons inside the solid kerogen affect the distribution of the produced hydrocarbons into gases and liquid products [21–23].

Studies using inductively coupled plasma optical emission spectroscopy (ICP-OES) have indicated that shale oil contains metals such as Fe, Mn, As, Pb, Ni, and Zn [17]. The presence of these elements in shale oil limits its usage as a fuel in engines. In a separate study by Dan et al. [24], using laser ablation inductively coupled plasma mass spectrometry (LA-ICP-MS), the authors reported the presence of 19 elements in oil shale and its solid waste. These elements include Mn, As, Pb, Ni, Zn, and many others. Unfortunately, these authors did not study the presence of metals in shale oil. The final pyrolysis temperature has an impact on the oil shale content of trace element migration. Trace element migration and volatility in semi-coke were studied as a function of final pyrolysis temperature, and it was found that higher migration indicated a higher rate of trace element transfer to gas and liquid phases. The migration of metals from coal during pyrolysis was found to be influenced by the pyrolysis conditions [25].

In this research work, the transfer of metals from oil shale during pyrolysis will be investigated. The transfer of elements will be studied as a function of the heating rate of oil shale during the pyrolysis process for some Jordanian oil shales.

2. Materials and methods

2.1. Oil shale pyrolysis

The oil shale sample was obtained from the Attarat Um Al-Ghudran area (31°16′08″ N, 36°26′52″ E). Chunk pieces were crushed in a jaw crusher to smaller sizes. The crushed samples were mixed and sieved to the desired size of 4 ± 1.5 mm. This step was performed to create a uniform composite sample that retained the homogeneity of the oil shale.

The proximate and ultimate analyses of the Attarat oil shale are shown in Table 1. The proximate analysis of the study sample indicates that 63.15 wt.%

Table 1. Proximate and ultimate analyses of Attarat oil shale

Proximate analysis components	**Ash**	**Volatile matter**	**Moisture**	**Fixed carbon**
wt.%	63.15	34.52	0.88	1.45
Ultimate analysis (elemental)	C	H	S	N
wt.%	17.89	1.75	3.02	2.76

of the sample is ash. The major composition of the ash is calcium oxide and silica, in addition to other minor components such as iron and aluminum oxides etc. [33]. The fixed carbon is the solid carbon that remains in the spent ash (unextractable carbon). According to elemental analysis, C accounts for 17.9 wt.%, followed by S at 3.02 wt.%, while N and H account for 2.76 and 1.75 wt.%, respectively.

The retort consisted of a stainless steel pipe with an inner diameter of 75 mm. The length of the retort was 300 mm. A special stainless steel perforated basket was fabricated and placed in the middle of the retort to contain the oil shale sample. A sample size of 300 g or more of oil shale was placed into the basket. The insulated retort was heated using an electrical heater wrapped around the stainless steel retort. The pyrolysis experiments were conducted at a final temperature of 550 °C. The heating rates were 5, 10, 15, and 20 °C/min. The temperature of the sample inside the retort was measured using type K thermocouple, and the process was regulated with a microcontroller (Arduino Uno) integrated into the system. Nitrogen gas flow rate was 200 mL/min, and the oil shale sample mass was approximately 300 g for each run. The hydrocarbon vapors were condensed using a circulating coolant operating at 5 °C or lower. The condensed shale oil, spent shale, and oil shale samples were subjected to metal detection and quantification using an inductively coupled plasma mass spectrometer (ICP-MS), specifically the Agilent 7500 model. The experimental work was performed in triplicate, and an overall material balance is indicated in Table 2. The masses of shale oil and water were measured together since it was not possible to separate the water from the shale oil due to the small amounts of water generated. It is clear from the data that oil yield fluctuations were heating-rate dependent. The mass of gases increased at the expense of shale oil with increasing heating rate.

Table 2. Pyrolysis variables and mass-balance results

Run No.	Heating rate, °C/min	Final temperature, °C	Mass of sample, g	Mass of shale oil and water, g	Mass of spent ash, g	Mass of non-condensable gases by difference, g	Oil yield, %
1		550	300	73	210	17	23.63
2	5	550	300	71	214	15	22.98
3		550	300	77	207	16	24.92
4		550	300	71	207	22	22.98
5	10	550	300	69	210	21	22.33
6		550	300	66	211	23	21.36

Continued on the next page

Table 2. *Continued*

Run No.	Heating rate, °C/min	Final temperature, °C	Mass of sample, g	Mass of shale oil and water, g	Mass of spent ash, g	Mass of non-condensable gases by difference, g	Oil yield, %
7		550	300	52	223	25	16.83
8	15	550	300	60	212	28	19.42
9		550	300	55	215	30	17.80
10		550	300	45	222	33	14.57
11	20	550	300	43	226	31	13.92
12		550	300	48	216	36	15.54

2.2. Sample preparation for metal analysis

To determine the metal content of the solid materials such as oil shale and spent shale after the pyrolysis process, acid digestion and metal extraction were conducted. A microwave digestion system (Ethos Easy, Milestone, Italy) with temperature feedback control up to 300 °C using a temperature sensor was employed. Oil shale was combusted at 950 °C to volatilize the different forms of water in oil shale, volatile matter, and the kerogen organic content. Tests were performed on particles of samples after grinding them using an Agate ball mill to pass 200 mesh (75 μm).

For each test sample, volumes of 6.0 to 12.0 mL of HNO_3, 1.0 to 3.0 mL of HF or 1.0 to 3.0 mL HCl, and 1.0 to 3.0 mL of H_2O_2 were added using a micropipette. The samples were mixed and transferred to the microwave digestion apparatus. A programmed method consisting of heating for 40 min to reach 230 °C, maintaining this temperature for 30 min, followed by cooling and centrifugation at 2000–3000 rpm for 10 min, was used. Upon completion, the sample was ready for ICP-MS analysis to determine the predefined metals, (Fe, Mn, Pb, Ni, and V).

The analysis of oil shale, spent shale, and shale oil samples, along with the determination of target metals (Fe, Mn, As, Pb, Ni, and V), was performed using an ICP-MS, specifically the Agilent 7500 model equipped with a Babington nebulizer due to the instrument's ability to perform multi-element analysis and to measure elements at trace levels. The specific conditions and parameters utilized during the ICP-MS analysis are outlined in Table 3. All measurements were carried out at the Jordan Atomic Energy Commission located in Amman, Jordan.

Table 3. Operating conditions and measurement parameters for ICP-MS

Parameter	Specification
Spectrometer	Agilent 7500 series ICP-MS
Nebulizer	Babington
Spray chamber	Quartz Scott-type
Mass analyzer	Quadrupole
Radio frequency power, kW	1330
Nebulizer gas flow, L/min	1
Auxiliary gas flow, L/min	1
Argon gas tank pressure, kPa	811

Measured mass/charge, m/z					
Fe	Mn	Ni	V	As	Pb
57	55	60	51	75	208

3. Results and discussion

Generally, oil shale is composed of organic and inorganic fractions that contain metals and rare earth elements [26], which are embedded in both fraction structures. For example, compounds such as $C_{20}H_{14}N_4Ni$ (nickel porphyrins, where the Ni atom is incorporated into the porphyrin framework [27]) and octaethyl nickel porphyrin ($C_{34}H_{44}N_4Ni$) [28] may be present. These compounds may exist in different forms such as the heavy fraction of shale oil, or organic extracts of oil shale, and could be associated with kerogen and bitumen in oil shale. On the other hand, V can also be present in different forms in crude oils and oil shale/shale oil, such as $C_{20}H_{12}N_4VO$ (vanadyl porphyrins), nitrogen heterocycles, or vanadium-asphaltene complexes either in the heavy fraction of shale oil or in bitumen [29]. As is present in crude oil and shale oil. Several authors have investigated the presence of As in crude and shale oils and reported the presence of methylated As compounds, AsH_2CH_3, $AsH(CH_3)_{2\text{-}3}$, and roxarsone (4-hydroxy-3-nitrophenylarsonic acid) ($C_6H_6AsNO_6$) [30]. Typical concentrations in shale oil ranged between a few ppm and more than 100 ppm [31, 32]. These authors claimed that thermally stable metal arsenide and metal arsenous sulfides are removed from shale oil by hydrocatalytic processing. The possibility of As solubility in the retorted water renders the spent catalyst as industrial waste.

The main interest in the present work is to trace the transfer of some metals from the oil shale solid material to shale oil and conduct an elemental material balance of the selected migrated elements during the pyrolysis process. The presence of metals such as Fe, Mn, Pb, Ni, and V could harm the operation of combustion engines.

The experimental runs were conducted for 300 g of fresh oil shale samples. A material balance was conducted on all runs since the spent shale, shale oil, and water liquids were collected, weighed, and the gas mass was calculated by difference. A material balance on the intended elements was also conducted (Table 4).

According to the results presented in Table 4, an elemental material balance using ICP-MS data is reported. The elemental mass balance was performed according to Eq. (1):

$$Metal\ mass\ (g) = sample\ mass\ (g) \times ppm \times 10^{-6}, \text{Eqs} \qquad (1)$$

$$\%\ recovery = \frac{(mass\ in\ spent\ \text{shale} + mass\ in\ shale\ oil)}{(mass\ in\ oil\ shale)} \times 100. \qquad (2)$$

The ICP-MS results for each investigated elemental metal, reported as ppm values, are presented in Table 4. These concentrations in ppm are used in Eq. (1) for calculating the metal mass. The mass of the sample (g) used in the equation is the average of triplicate tests using ICP-MS. According to this average value, the percentage recovery is calculated. Since the heating rate is thought to play a role in the rate of metal transfer to shale oil, the data in Table 4 are also presented as a function of heating rate. Before discussing the transfer of metals from oil shale to liquid, tests were conducted to determine the metal content of the oil shale rock. In Table 4, the metal content of the oil shale sample material indicates that the concentrations in ppm for V, Mn, Ni, As, Pb, and Fe are 342.2, 21.28, 171.76, 18.38, 3.26, and 2969, respectively. As clearly presented in column 6 of Table 4, the percentage recovery (mass balance) calculated according to Eq. (2) for these metals fluctuated between 76.9% for V and 109.3% for Fe. These elemental mass balances are reported without any manipulations or alterations of the experimental findings. The ppm readings obtained by ICP-MS are substituted directly into Eq. (1) to obtain the elemental mass balances. These results are based on the original charged oil shale sample of 300 g. The percentage recovery of V is the lowest among all studied elements and ranges from 76.9 to 86.3%, although V has the lowest atomic weight (50.94). This low recovery could be due to a low rate of metal transfer to shale oil. As it can be calculated from Table 4, the transfer of V to shale oil is < 0.52% of the original oil shale sample.

Table 4. V, Mn, Ni, As, Pb, and Fe concentrations in oil shale and spent shale as a function of heating rates

Mass concentrations, ppm					Metal recovery, %	Heating rate, °C/min
Metal / atomic weight	Oil shale	Spent shale	Shale oil	Gases		
V/50.94	342.2	390.8	1.1	0	78.4	5
		376.6	1.6	0	76.9	10
		371.7	0.8	0	78.5	15
		400.0	1.8	0	86.3	20
Mn/54.94	21.3	28.7	< 1	0	86.8	5
		29.0	< 1	0	94.9	10
		25.1	< 1	0	85.0	15
		24.6	< 1	0	85.4	20
Ni/58.69	171.8	208.9	5.5	0	81.5	5
		199.7	6.0	0	81.9	10
		197.9	3.4	0	84.0	15
		195.3	3.1	0	84.1	20
As/74.92	18.4	18.4	10.1	0	84.0	5
		17.2	13.9	0	82.7	10
		17.6	12.2	0	81.3	15
		17.5	11.0	0	79.3	20
Pb/207.2	3.3	4.5	< 1	0	88.3	5
		4.0	< 1	0	85.2	10
		4.1	< 1	0	90.4	15
		4.0	< 1	0	90.8	20
Fe/56.8	2969	4501.7	59.4	0	93.6	5
		3977.0	35.7	0	93.7	10
		4482.7	34.1	0	109.3	15
		4162.3	25.3	0	103.5	20

As evident in Table 4, the transfer of V to shale oil did not show a clear trend with the heating rates studied, although it decreased with increased rates of 10 and 15 °C/min and then increased at 20 °C/min. The largest percentage recovery was observed for Fe, fluctuating between 93.6% and 109.3%. It should be noted that the Fe concentration in the oil shale sample is high, reaching 0.3% of the total oil shale mass.

3.1. Spent shale

Figure 1(a) presents the concentrations of V, Ni, and Fe in the spent shale. Calculating the average metal percentages for V, Ni, and Fe that remained in the spent shale considering the studied heating rates gives values of 79.94%, 82.22%, and 99.75%, respectively.

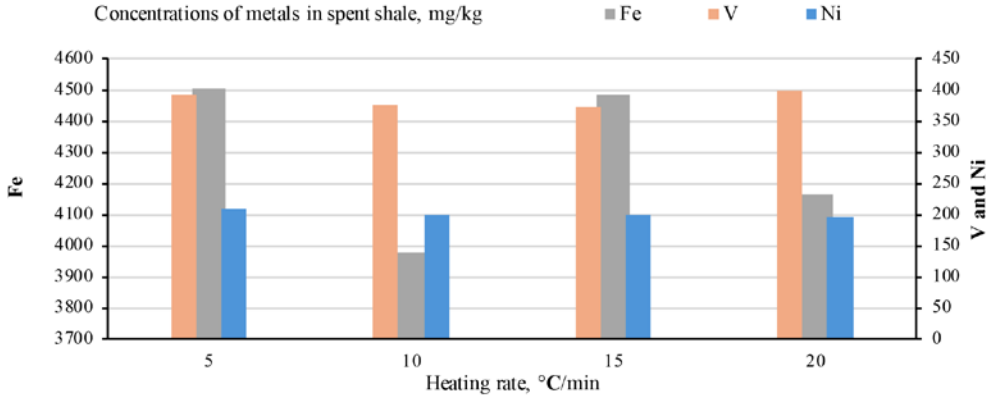

Fig. 1(a). Concentrations of metals in spent shale, ppm.

The concentration of Ni in oil shale is 171.76 ppm, and the concentration remaining in the spent shale is 197.6 ppm. These figures indicate that 82.22% of Ni is not transferred and remains in the solid material. Similarly, from Fig. 1(a), the concentration of Fe remaining in the spent shale is 99.75% of the original oil shale content.

The transfer of Mn to shale oil from oil shale during pyrolysis is < 1 ppm and the concentration of Mn remaining in the spent shale is 88.04% based on Table 4 data for material balance calculations. From Fig. 1(a) and the material balance calculations, no definite relationship exists between the heating rate and the concentrations of these elements remaining in the spent shale.

The concentrations of Mn, As, and Pb in the spent shale after pyrolyzing oil shale are depicted in Fig. 1(b). The concentrations of these elements fluctuate between 24.63–28.97, 17.24–18.5, and 3.98–4.08 ppm, respectively. These values do not show any relationship between the concentrations of these metals remaining in the spent shale and the heating rates. The average

percentage of Mn remaining in the spent shale according to the mass balance in Table 4 is 88.04%, while the average percentage of As and Pb in spent shale are 68.78% and 88.67%, respectively.

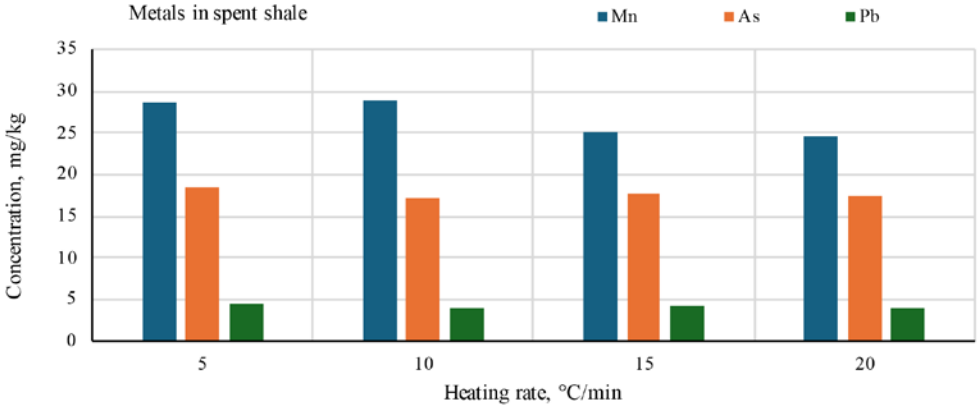

Fig. 1(b). Concentrations of metals in spent shale, ppm.

3.2. Shale oil

The concentrations of Fe, V, Ni, and As in shale oil are depicted in Fig. 2. The concentrations of Mn and Pb are not reported since their concentrations as detected by ICP-MS are <1 ppm. The maximum concentration of Fe is 59.4 ppm in shale oil as reported at a heating rate of 5 °C/min and depicted in Fig. 2. The concentrations of Fe in shale oil at 10, 15, and 20 °C/min are 35.69, 34.14, and 25.29 ppm, respectively. These concentrations show a decreasing trend with increasing heating rates. The concentrations of V are 1.1, 1.5, 0.8,

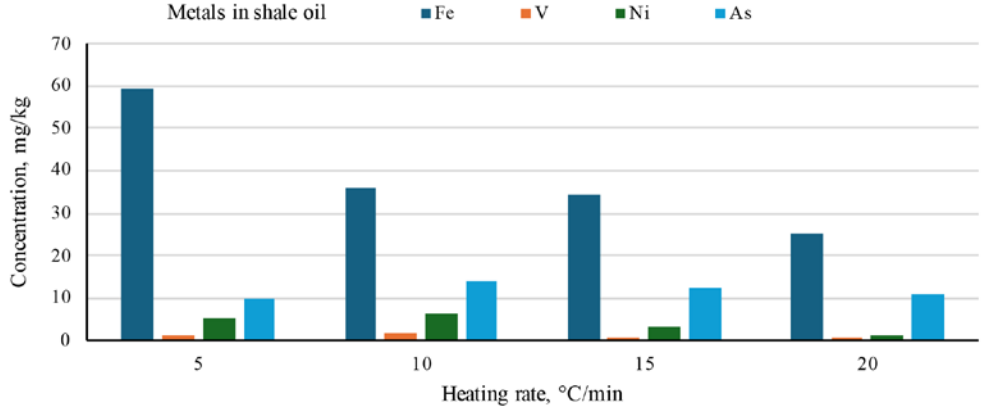

Fig. 2. Concentrations of metals in shale oil, ppm.

and 1.8 ppm at 5, 10, 15, and 20 °C/min, respectively. At a heating rate of 5 °C/min, the concentrations of Ni and As are 5.5 and 10.1 ppm, respectively, while at 10 °C/min, the corresponding concentrations are 6.0 and 13.9 ppm. At 15 °C/min, the concentrations of Ni and As are 3.4 and 12.2 ppm, respectively. Finally, at 20 °C/min, the corresponding concentrations are 3.1 and 11.0 ppm. These concentrations for Fe, V, Ni, and As represent 0.277%, 0.0740%, 0.56%, and 0.0134% of the total content of shale oil, respectively. In general, there is no clear trend relating to metal concentrations in shale oil with the heating rate.

4. Conclusions

The transfer of certain metals embedded in oil shale to shale oil during pyrolysis was investigated for Attarat oil shale. It has been proved that Fe, V, Ni, Mn, Pb, and As are transferable during pyrolysis. The elemental mass balances have shown acceptable values. The recovery of these elements (transferred to shale oil and remaining in the spent shale) varied between 76.9% for V and 109.26% for Fe. The transferred mass of these elements did not show a clear trend with 5, 10, 15, and 20 °C/min heating rates. Some increasing and decreasing trends were observed for some elements with consecutive heating rate values. The lower values of metal concentrations in shale oil could be influenced by other inputs or reaction conditions. Further investigations are required to assess the transfer of metals present in oil shale at higher heating rates, different final pyrolysis temperatures, and probably different reaction environments such as helium, carbon dioxide, and hydrogen gas, as well as particle size and the subsequent diffusional influences on reaction kinetics and kerogen decomposition, as recommended by previous researchers.

Data availability statement

All data used in this article are publicly available. No new data were created or analyzed in this study.

Acknowledgments

The authors acknowledge the support and assistance of the Jordan Atomic Energy Commission for analyzing the samples. The publication costs of this article were covered by the Estonian Academy of Sciences.

References

1. Al-Ayed, O. S., Suliman, M. R., Rahman, N. A. Kinetic modeling of liquid generation from oil shale in fixed bed retort. *Applied Energy*, 2010, **87**(7), 2273–2277. https://doi.org/10.1016/j.apenergy.2010.02.006
2. Wang, S., Jiang, A., Han, X., Tong, J. Effect of residence time on products yield and characteristics of shale oil and gases produced by low-temperature retorting of Dachengzi oil shale. *Oil Shale*, 2013, **30**(4), 501–516. https://doi.org/10.3176/oil.2013.4.04
3. Pan, L., Dai, F., Pei, S., Huang, J., Liu, S. Influence of particle size and temperature on the yield and composition of products from the pyrolysis of Jimsar (China) oil shale. *Journal of Analytical and Applied Pyrolysis*, 2021, **157**, 105211. https://doi.org/10.1016/j.jaap.2021.105211
4. Wallman, P. H., Tamm, P. W., Spars, B. G. Oil shale retorting kinetics. In *Oil Shale, Tar Sand, and Related Materials* (Stauffer, H. C., ed.). American Chemical Society, Washington, 1981, 93–113.
5. Trejo, F., Ancheyta, J., Centeno, G., Marroquín, G. Effect of hydrotreating conditions on Maya asphaltenes composition and structural parameters. *Catalysis Today*, 2005, **109**(1–4), 178–184. https://doi.org/10.1016/j.cattod.2005.08.013
6. Ancheyta, J., Centeno, G., Trejo, F., Marroquín, G. Changes in asphaltene properties during hydrotreating of heavy crudes. *Energy & Fuels*, 2003, **17**(5), 1233–1238. https://doi.org/10.1021/ef030023
7. Amer, M. W., Alhesan, J. S. A., Marshall, M., Awwad, A. M., Al-Ayed, O. S. Characterization of Jordanian oil shale and variation in oil properties with pyrolysis temperature. *Journal of Analytical and Applied Pyrolysis*, 2019, **140**, 219–226. https://doi.org/10.1016/j.jaap.2019.03.019
8. Zuo, P., Qu, S., Shen, W. Asphaltenes: separations, structural analysis and applications. *Journal of Energy Chemistry*, 2019, **34**, 186–207. https://doi.org/10.1016/j.jechem.2018.10.004
9. Oja, V., Rooleht, R., Baird, Z. S. Physical and thermodynamic properties of kukersite pyrolysis shale oil: literature review. *Oil Shale*, 2016, **33**(2), 184–197. https://doi.org/10.3176/oil.2016.2.06
10. Al-Jaraden, T., Ayadi, O., Alahmer, A. Towards sustainable shale oil recovery in Jordan: an evaluation of renewable energy sources for in-situ extraction. *International Journal of Thermofluids*, 2023, **20**, 100446. https://doi.org/10.1016/j.ijft.2023.100446
11. Ibrahim, K. M., Rahman, H. A. Geochemistry and mineralogy of oil shale from Attarat Umm Ghudran area, Jordan. *Advance Engineering Science*, 2023, **55**(1), 3209–3229.
12. Hamarneh, Y. *Oil Shale Resources Development in Jordan*. Ministry of Energy and Mineral Resources, Natural Resources Authority, 1998.
13. Ibrahim, K. M., Aljurf, S., Rahman, H. B. A., Gülamber, C. Exploration and evaluation of oil shale resources from Attarat area, central Jordan. In *IMCET 2019*, 16–19 April 2019, Antalya, Turkey, 1116–1128.

14. El-Hasan, T., Abu-Jaber, N., Abdelhadi, N. Hazardous toxic elements mobility in burned oil shale ash and attempts to attain short- and long-term solidification. *Oil Shale*, 2019, **36**(2S), 226–249. https://doi.org/10.3176/oil.2019.2S.12
15. Al-Ayed, O. S., Hajarat, R. A. Shale oil: its present role in the world energy mix. *Global Journal of Energy Technology Research Updates*, 2018, **5**, 11–18. https://doi.org/10.15377/2409-5818.2018.05.2
16. Al-Ayed, O. S., Kunzru, D. Cyclohexane dehydrogenation on a nickel catalyst: kinetics and catalyst fouling. *Journal of Chemical Technology and Biotechnology*, 1988, **43**(1), 23–38. https://doi.org/10.1002/jctb.280430104
17. Abu-Nameh, E. S. M., Al-Ayed, O. S., Jadallah, A. Determination of selected elements in shale oil liquid. *Oil Shale*, 2019, **36**(2S), 179–187. https://doi.org/10.3176/oil.2019.2S.08
18. Wang, H., Zhang, W., Qiu, S., Liang, X. Release characteristics of Pb and BETX from in situ oil shale transformation on groundwater environment. *Scientific Reports*, 2021, **11**, 16166. https://doi.org/10.1038/s41598-021-95509-2
19. Liu, P., Li, W., Tan, R., Zhongbin, L, Bin, Z. Investigation of pyrolysis behavior shale gas oil-based drilling cuttings kinetics and product characteristics. *Scientific Reports*, 2025, **15**, 19775. https://doi.org/10.1038/s41598-025-04640-x
20. Bai, J. R., Song, K. T., Chen, J. B. The migration of heavy metal elements during pyrolysis of oil shale in Mongolia. *Fuel*, 2018, **225**, 381–387. https://doi.org/10.1016/j.fuel.2018.03.168
21. Zhang, Y., Guan, J., Qiao, P., Li, J., Zhang, W. Effects of secondary reaction of primary volatiles on oil/gas yield and quality in oil shale pyrolysis. *Journal of Fuel Chemistry and Technology*, 2021, **49**(7), 924–932. https://doi.org/10.1016/S1872-5813(21)60046-4
22. Zhan, H., Qin, F., Chen, S., Chen, R., Meng, Z., Miao, X. et al. Two-step pyrolysis degradation mechanism of oil shale through comprehensive analysis of pyrolysis semi-cokes and pyrolytic gases. *Energy*, 2022, **241**, 122871. https://doi.org/10.1016/j.energy.2021.122871
23. Huang, Y., Zhang, M., Lyu, J., Yang, H., Liu, Q. Modeling study on effects of intraparticle mass transfer and secondary reactions on oil shale pyrolysis. *Fuel*, 2018, **221**, 240–248. https://doi.org/10.1016/j.fuel.2018.02.076
24. Yang, D., Tanilas, K., Konist, A., Järvik, O. Evaluating LA-ICP-MS and digestion-based ICP-MS methods for trace elements determination in oil shale and its solid wastes. *Talanta*, 2025, **295**, 128319. https://doi.org/10.1016/j.talanta.2025.128319
25. Quann, R. J., Neville, M., Janghorbani, M., Mims, C. A., Sarofim, A. F. Mineral matter and trace-elements vaporization in a laboratory-pulverized coal combustion system. *Environmental Science & Technology*, 1982, **16**(11), 776–781. https://doi.org/10.1021/es00105a009
26. Al-Ayed, O. S., Qawaqneh, M. K., Abu-Nameh, E. S. M. Tracing rare earth elements in oil shale ash. *Oil Shale*, 2024, **41**(2), 132–143. https://doi.org/10.3176/oil.2024.2.04

27. Habib, A., Serniabad, S., Khan, M. S., Islam, R., Chakraborty, M., Nargis, A. et al. Kinetics and mechanism of formation of nickel (II)porphyrin and its interaction with DNA in aqueous medium. *Journal of Chemical Science*, 2012, **133**, 83. https://doi.org/10.1007/s12039-021-01945-y
28. Stasiuk, R., Matlakowska, R. Postdiagenetic bacterial transformation of nickel and vanadyl sedimentary porphyrins of organic-rich shale rock (Fore-Sudetic Monocline, Poland). *Frontiers in Microbiological Chemistry and Geomicrobiology*, 2021, **12**, 772007. https://doi.org/10.3389/fmicb.2021.772007
29. Yakubov, M., Abilova, G., Tazeeva, E., Yakubova, S., Tazeev, D., Mironov, N. et al. A comparative analysis of vanadyl porphyrins isolated from resins of heavy oils with high and low vanadium content. *Processes*, 2021, **9**(12), 2235. https://doi.org/10.3390/pr9122235
30. O'Day, P. A. Chemistry and mineralogy of arsenic. *Elements*, 2006, **2**(2), 77–83. https://doi.org/10.2113/gselements.2.2.77
31. Sikonia, J. G. Arsenic management in shale oil upgrading. Environmental Geochemistry and Health, 1985, **7**, 64–68. https://doi.org/10.1007/BF01771340
32. Al-Ayed, O. S., Al-Harahsheh, A., Khaleel, A. M., Al-Harahsheh, M. Oil shale pyrolysis in fixed-bed retort with different heating rates. *Oil Shale*, 2009, **26**(2), 139–147. https://doi.org/10.3176/oil.2009.2.06
33. Voolmaa, M., Soesoo, A., Puura, V., Hade, S., Aosaar, H. Assessing the geochemical variability of oil shale in the Attarat Um Ghudran deposit, Jordan. *Estonian Journal of Earth Sciences*, 2016, **65**(2), 61–74. https://doi.org/10.3176/earth.2016.06